


Journal of
***Mechanics of
Materials and Structures***

**EFFECT OF AIR GAPS ON THE BALLISTIC
RESISTANCE OF DUCTILE SHIELDS PERFORATED
BY NONCONICAL IMPACTORS**

Gabi Ben-Dor, Anatoly Dubinsky and Tov Elperin

Volume 1, Nº 2

February 2006

 mathematical sciences publishers

EFFECT OF AIR GAPS ON THE BALLISTIC RESISTANCE OF DUCTILE SHIELDS PERFORATED BY NONCONICAL IMPACTORS

GABI BEN-DOR, ANATOLY DUBINSKY AND TOV ELPERIN

In *Int. J. Solids Struct.* **35**:23 (1998), pp. 3097–3103, we proved that localized interaction model (LIM) for shield-impactor interaction implies independence of the ballistic limit velocity (BLV) of spaced shield on air gaps and their widths for conical striker. In this study, the effect of deviation from a conical shape on ballistic properties of spaced shield is investigated using two-term LIM. It is found that this effect is insignificant and it causes small changes (of the order of few percent) in the magnitude of the BLV and energy absorbed by a shield. These theoretical predictions are in agreement with the available experimental results.

1. Introduction

Currently there is no consensus on the effect of layering and spacing on the ballistic properties of shields, although interest in this topic has existed for a long time.

Hurlich [1950] noted that the earliest study he found on the modern use of spaced armor was performed in 1913 for armor of naval vessels. He presented some qualitative arguments in favor of spaced armor (mostly for tanks), a number of tables with experimental results, some references and curious historical information. Honda et al. [1930] investigated experimentally the impact of steel plates by conical-nosed projectiles. It was found that a spaced shield with thicknesses of the plates equal to the half-thickness of a monolithic shield performed better than a monolithic shield. Marom and Bodner [1979] conducted a combined analytical and experimental comparative study of monolithic, layered and spaced thin aluminum shields. They found that the ballistic resistance of a monolithic shield is higher than that of a multilayered shield with the plates in contact and lower than the ballistic resistance of a spaced shield. Radin's study [1988] was also based on semi-empirical models and experimental investigations. They found a monolithic aluminum shield to be superior to a layered shield with the same total thickness for conical-nose and blunt projectiles, while spaced shields were less effective. Zukas [1996] performed calculations with thick plates impacted by long rod projectiles

Keywords: localized interaction model, ballistic limit velocity, spaced shield, nonconical impactor.

moving at 1500 m/s. The calculations showed that air gaps of one and four projectile diameters between plates involved the increase of projectile residual velocity when compared to their monoblock equivalent and a shield consisting of plates in contact. The sizes of the gaps play a minor role in determining the residual velocity. Using experimental results obtained for aluminum and steel plates and armor-piercing projectiles, Gupta and Madhu [1997] found that for the same impact velocity the residual velocity for the spaced shield was larger than for the plates in contact. Corran [1983a; 1983b], using experimental results on penetration of mild steel plates by impactors having “increasingly rounded nose shape”, presented some data on perforation energy of spaced shields. Almohandes et al. [1996] conducted a comprehensive experimental study on the perforation of mild steel by standard 7.62 mm bullets. They investigated layered in contact, spaced and monolithic shields with total thickness in the range 8–14 mm. The efficiencies of shields were assessed by comparing their residual velocities for the same magnitude of the impact velocity. Almohandes’ experimental results were used by Liang et al. [2005] for validating their penetration model. Applying this model for comparative analysis of shields with different structures, they concluded that an air gap slightly influenced the resistance to perforation in multilayered shields. Elek et al. [2005] developed a simple model to describe the perforation of monolithic and multilayered thin metallic plates by a flat-ended cylindrical impactor and used their model for the analysis of the ballistic properties of multilayered spaced shields. The main results of this study may be summarized as follows. The suggested model predicted that the monolithic shield will have larger resistance than any other multilayered shield with standoff distance between layers and equivalent total mass. The analysis of penetration in a two-layered shield showed that the maximum resistance could be obtained for very low or very high first-layer thickness (less than 20% or more than 80% of total thickness). The increase of the number of spaced layers of a multilayered shield, at constant total mass, caused a further decrease of the ballistic resistance.

In [Ben-Dor et al. 1998b; 1998a; 1999], we studied analytically the influence of air gaps between the plates on the ballistic limit velocity (BLV) of a multilayered shield. Using the general localized interaction model (LIM). In the first of these articles we found that the ballistic performance of the shield against 3D conical-nosed impactors is independent of the widths of the air gaps and of the sequence of plates in the shield and that it is determined only by the total thickness of the plates if the plates are manufactured from the same material. The influence of air gaps on the BLV of a shield that consisted of two plates manufactured from different materials was studied in [Ben-Dor et al. 1999] using the two-term localized interaction model. They found the criterion (depending on mechanical properties of the materials of the plates) that governs the decrease or the increase of the BLV

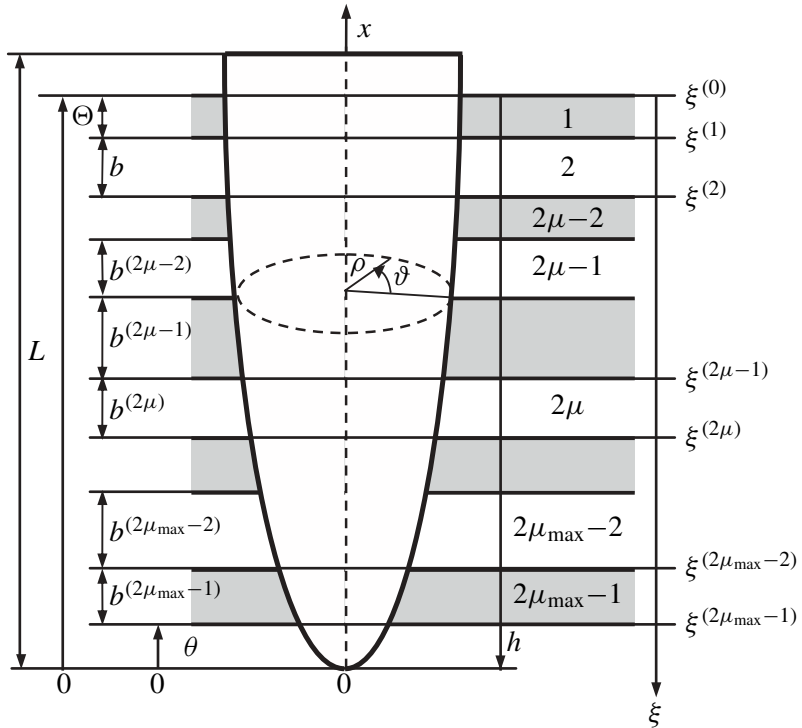


Figure 1. Notations.

of the shield with increasing the air gap thickness. Using the cylindrical cavity expansion model, we studied in [Ben-Dor et al. 1998a] the effect of air gaps on the ballistic performance of a spaced shield comprising plates manufactured from the same material and found that the BLV of the shield slightly increased with the increase of the widths of air gaps. In this study we investigate the effect of air gaps on ballistic properties of shields against nonconical impactors.

2. Formulation of the problem

Consider a high speed normal penetration of a rigid sharp striker (a body of revolution) into a ductile spaced shield with a finite thickness. We assume that the conditions of penetration are determined mainly by the “ductile hole enlargement perforation mechanism” ([Backman and Goldsmith 1978]). The basic notations are shown in Figure 1, and it is assumed that only the nose of the cylindrical impactor can interact with the shield. The coordinate h , the instantaneous depth of penetration, is defined as the distance between the leading edge of the nose of the impactor and the rear surface of the shield. The coordinate ξ is associated with the shield. In cylindrical coordinates (x, ρ, ϑ) associated with the impactor, the

surface of the nose is described by the equation

$$\rho = \phi(x), \quad 0 \leq x \leq L, \quad 0 \leq \vartheta \leq 2\pi,$$

where L is the length of the impactor's nose and $\Phi(x)$ is an increasing convex function. Assume that the shield consists of $2\mu_{\max} - 1$ layers including μ_{\max} plates with the thicknesses $b^{(1)}, b^{(3)}, \dots, b^{(2\mu_{\max}-1)}$ and air gaps between the plates with the thicknesses $b^{(2)}, b^{(4)}, \dots, b^{(2\mu_{\max}-2)}$. The plate with number $2\mu - 1$ is located between the cross-sections $\xi = \xi^{(2\mu-2)}$ and $\xi = \xi^{(2\mu-1)}$, where $\mu = 1, 2, \dots, \mu_{\max}$ and $\xi^{(0)} = 0$. The total thickness of the shield (the sum of the thicknesses of all layers including the air gaps) and the sum of the thickness of all plates are denoted b and b_{sum} , respectively. It is assumed that the plates are manufactured from the same material. The part of the lateral surface of the impactor between the cross-sections $x = \theta(h)$ and $x = \Theta(h)$ (see Figure 1) interacts with some layers of the shield or is in contact with some air gaps (see Figure 2, top):

$$\theta(h) = \begin{cases} 0 & \text{if } 0 \leq h \leq b, \\ h - b & \text{if } b \leq h \leq b + L, \end{cases} \quad \Theta(h) = \begin{cases} h & \text{if } 0 \leq h \leq L, \\ L & \text{if } h \geq L. \end{cases}$$

The equation of motion of the impactor, $m(d^2h/dt^2) = -D$, can be rewritten as

$$mv(dv/dh) = -D, \tag{1}$$

where the velocity of the impactor v is considered to be a function of h , m is the mass of the impactor, and D is the resistance force. We consider the range of impact velocities v_{imp} whereby the projectile perforates the shield. Perforation occurs when the position of the striker is $h = b + L$. The ballistic limit velocity v_{bl} is defined as the impact velocity of the impactor required to emerge from the shield with zero residual velocity, $v_{\text{res}} = 0$.

We assume that the impactor-target interaction at a given location at the surface of the impactor that is in contact with a plate can be represented as

$$d\vec{F} = (\gamma(-\vec{v}^0 \cdot \vec{n}^0)^2 v^2 + \sigma)\vec{n}^0 dS, \tag{2}$$

where $d\vec{F}$ is the force acting at the surface element dS of the impactor, \vec{n}^0 is the inner normal unit vector at a given location on the impactor's surface, \vec{v}^0 the unit vector of the impactor's velocity, the parameters γ and σ depend on the properties of the material of the shield. Equation (2) comprises most of the widely used phenomenological models for homogenous shields (see [Recht 1990; Ben-Dor et al. 2005] for details). In particular, in the model proposed and validated in comprehensive experimental studies in [Vitman and Stepanov 1959], σ and γ are the ‘‘dynamical hardness’’ and material density of the shield, respectively. The values of these parameters for some materials are given in [Vitman and Ioffe 1948,

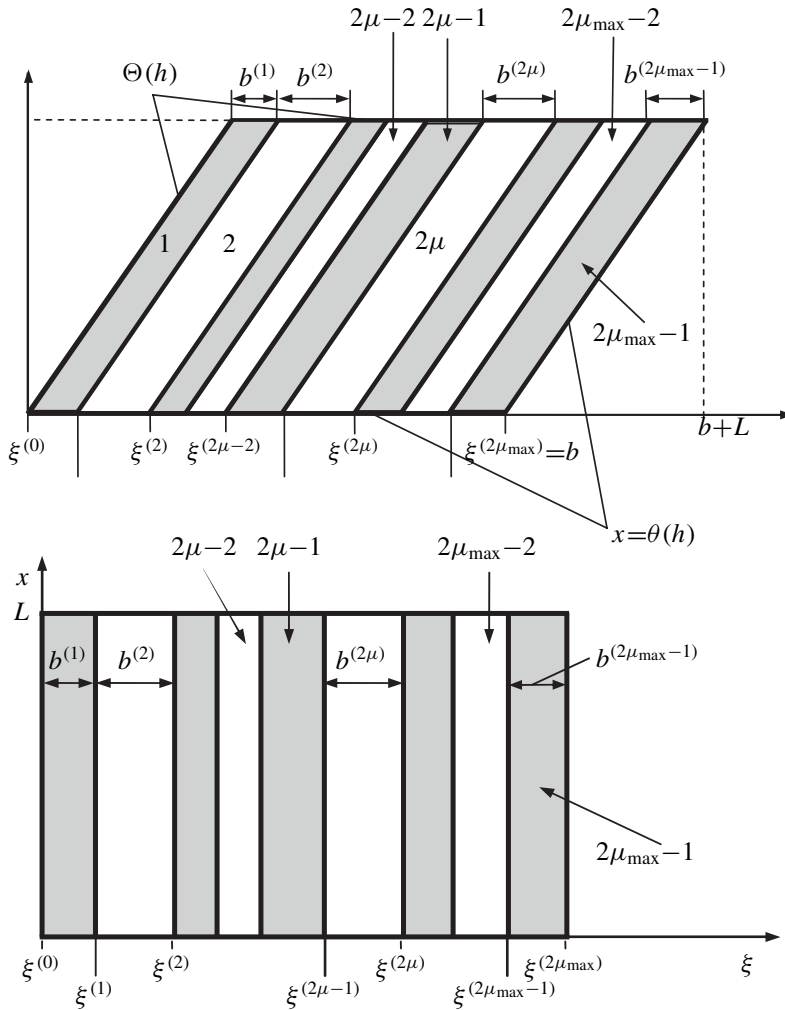


Figure 2. Model of the spaced shield, before and after a change of variables.

Table 1]. The remark by Recht [1990] concerning similar semi-empirical models is confirmed in this case: the parameter σ is significantly larger than the compressive yield strength.

In order to adapt (2) for a spaced shield we define a function $\varepsilon(\xi)$, which is equal to 1 if the point with the coordinate ξ (Figure 1) is located in any plate and is equal to 0 if this point is located in an air gap:

$$\begin{aligned} \varepsilon(\xi) &= \varepsilon^{(j)} \text{ if } \xi^{(j-1)} \leq \xi \leq \xi^{(j)}, \quad j = 1, 2, \dots, \mu_{\max} - 1, \\ \varepsilon^{(1)} &= \dots = \varepsilon^{(2\mu-1)} = \dots = \varepsilon^{(2\mu_{\max}-1)} = 1, \\ \varepsilon^{(2)} &= \dots = \varepsilon^{(2\mu)} = \dots = \varepsilon^{(2\mu_{\max}-2)} = 0. \end{aligned}$$

Then (2) can be rewritten as

$$d\vec{F} = \varepsilon(\xi)(\gamma(-\vec{v}^0 \cdot \vec{n}^0)^2 v^2 + \sigma)\vec{n}^0 dS.$$

The total force \vec{F} for some location of the impactor inside the shield is found by integrating the local force over the impactor-shield contact surface area, formally including the air gaps, that is, over the portion of the impactor's surface S determined by the inequalities $0 \leq \vartheta \leq 2\pi$ and $\theta(h) \leq x \leq \Theta(h)$. Taking into account the identity

$$\xi = h - x,$$

using the differential geometry formulas

$$-\vec{v}^0 \cdot \vec{n}^0 = \Phi' / \sqrt{\Phi'^2 + 1}, \quad dS = \sqrt{\Phi'^2 + 1} dx dv, \quad \Phi' = d\Phi/dx,$$

we obtain for the drag force D the expression

$$\begin{aligned} D &= \vec{F} \cdot (-\vec{v}^0) = \iint_S \varepsilon(\xi)(\gamma(-\vec{v}^0 \cdot \vec{n}^0)^2 v^2 + \sigma)(-\vec{v}^0 \cdot \vec{n}^0) dS \\ &= \frac{m}{2}(f_2(h)v^2 + f_0(h)), \end{aligned} \quad (3)$$

where

$$f_2(h) = \frac{4\pi\gamma}{m} \int_{\theta(h)}^{\Theta(h)} \frac{\varepsilon(h-x)\Phi\Phi'^3}{\Phi'^2 + 1} dx, \quad f_0(h) = \frac{4\pi\sigma}{m} \int_{\theta(h)}^{\Theta(h)} \varepsilon(h-x)\Phi\Phi' dx.$$

Substituting D from (3) into (1) we obtain, after some algebra, an ordinary linear differential equation with respect to v^2 :

$$dv^2/dh + f_2(h)v^2 + f_0(h) = 0.$$

The solution of this equation with the initial condition $v(0) = v_{\text{imp}}$, which corresponds to the beginning of the motion of the impactor with the impact velocity v_{imp} reads

$$v^2(h) = \frac{1}{q(h)}(v_{\text{imp}}^2 - g(h)), \quad (4)$$

(see [Kamke 1959]), where

$$q(h) = \exp\left(\int_0^h f_2(\eta) d\eta\right), \quad g(h) = \int_0^h f_0(H)q(H)dH.$$

Equation (4) yields formulas for the residual velocity, $v_{\text{res}} = v(b+L)$, and the ballistic limit velocity, v_{bl} :

$$v_{\text{res}}^2 = \frac{1}{q(b+L)}(v_{\text{imp}}^2 - g(b+L)), \quad v_{\text{bl}}^2 = g(b+L). \quad (5)$$

We now prove that $q(b + L)$ does not depend on the widths of the air gaps. To this end, we change the variables (Figure 2, bottom), $x \rightarrow x, h \rightarrow x + \xi$, in the integral in the expression for $q(b + L)$:

$$\begin{aligned} \frac{m}{4\pi\gamma} \ln(q(b + L)) &= \int_0^{b+L} dh \int_{\theta(h)}^{\Theta(h)} \varepsilon(h - x) \psi(x) dx \\ &= \int_0^L \psi(x) dx \int_0^b \varepsilon(\xi) d\xi = b_{\text{sum}} \int_0^L \psi(x) dx, \end{aligned}$$

where $\psi(x) = \Phi\Phi^3/(\Phi^2 + 1)$.

For further analysis it is convenient to rewrite the expression for v_{bl} in dimensionless variables where L is chosen as a characteristic length:

$$v_{\text{bl}} = \sqrt{\chi} \Psi(\alpha), \tag{6}$$

where function Ψ depends also on structure of the shield and the shape of the impactor, and

$$\begin{aligned} \Psi(\alpha) &= \sqrt{\alpha \int_0^{\bar{b}+1} Q(\bar{h}) d\bar{h} \int_{\bar{\theta}(\bar{h})}^{\bar{\Theta}(\bar{h})} \bar{\varepsilon}(\bar{h} - \bar{x}) \bar{\Phi} \bar{\Phi}' d\bar{x}}, \\ \alpha &= \frac{4\pi L^3}{m} \gamma, \quad \bar{x} = \frac{x}{L}, \quad \bar{\Phi} = \frac{\Phi}{L}, \quad \bar{\Phi}' = \frac{d\bar{\Phi}}{d\bar{x}}, \quad \bar{h} = \frac{h}{L}, \\ Q(\bar{h}) &= \exp\left(\alpha \int_0^{\bar{h}} d\bar{H} \int_{\bar{\theta}(\bar{H})}^{\bar{\Theta}(\bar{H})} \frac{\bar{\varepsilon}(\bar{H} - \bar{x}) \bar{\Phi} \bar{\Phi}'^3}{\bar{\Phi}^2 + 1} d\bar{x}\right), \quad \bar{\varepsilon}(\bar{\xi}) = \varepsilon(L\bar{\xi}), \\ \bar{\theta}(\bar{h}) &= \begin{cases} 0 & \text{if } 0 \leq \bar{h} \leq \bar{b}, \\ \bar{h} - \bar{b} & \text{if } \bar{b} \leq \bar{h} \leq \bar{b} + 1, \end{cases} \quad \bar{\Theta}(\bar{h}) = \begin{cases} \bar{h} & \text{if } 0 \leq \bar{h} \leq 1, \\ 1 & \text{if } \bar{h} \geq 1. \end{cases} \end{aligned}$$

Let v_{bl}^0 be the BLV of the shield that consists of the plates in contact with the same total thickness b_{sum} . Clearly, the latter structure is equivalent to a monolithic shield with the total thickness b_{sum} . Equation (6) implies that the ratio $\delta = v_{\text{bl}}/v_{\text{bl}}^0$ depends on the dimensionless parameter α as well as on the shape of the impactor and the dimensionless thicknesses of the layers (plates and air gaps). In our previous investigation it was found that spacing does not affect ballistic properties of shields against conical impactors [Ben-Dor et al. 1998b]. In the next section, using the obtained expression for the BLV we study numerically the effect of spacing on the BLV of the shields for nonconical impactors.

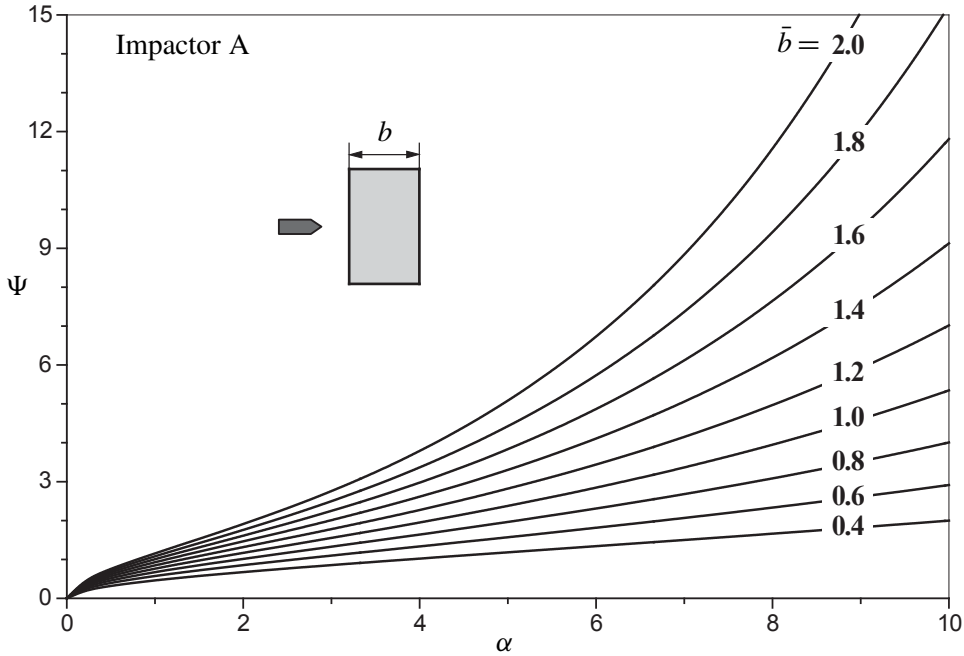


Figure 3. Function $\Psi(\alpha)$ for different values of \bar{b} .

3. Result of numerical calculations and discussion

We performed calculations for two impactors (cylindrical bodies of revolution with different nose shapes). The first impactor (Impactor A) is the cylinder with a semi-spherical nose. The generatrix of the nose of the second impactor (Impactor B) is the broken line consisting of segments between three points with the dimensionless coordinates $(\bar{x}, \bar{\rho})$: $(0, 0)$; $(0.3, 0.7)$; $(1, 1)$. The validity of this model for blunt, thick impactors against shield with a finite thickness is questionable, and, consequently, Impactor A can be considered only as a model.

In the following analysis, we use dimensionless variables. We show in Figure 3 plots of function Ψ for a monolithic plate. Using (6), one can determine the ranges of variation of parameters \bar{b}_{sum} and α that correspond to a given range of BLVs for a shield manufactured from a given material (for some materials one can use Table 1). The plots in Figure 3 correspond to Impactor A, and they differ only insignificantly from those obtained for Impactor B.

The top halves of Figures 4–10 correspond to Impactor A, while the bottom parts correspond to Impactor B.

Figure 4 shows the dependence of the parameter $\delta = v_{\text{bl}}/v_{\text{bl}}^0$ versus α for different widths of the gap (case with two plates). Inspection of these figures shows that ballistic efficiency of the shield decreases when the width of the gap between the

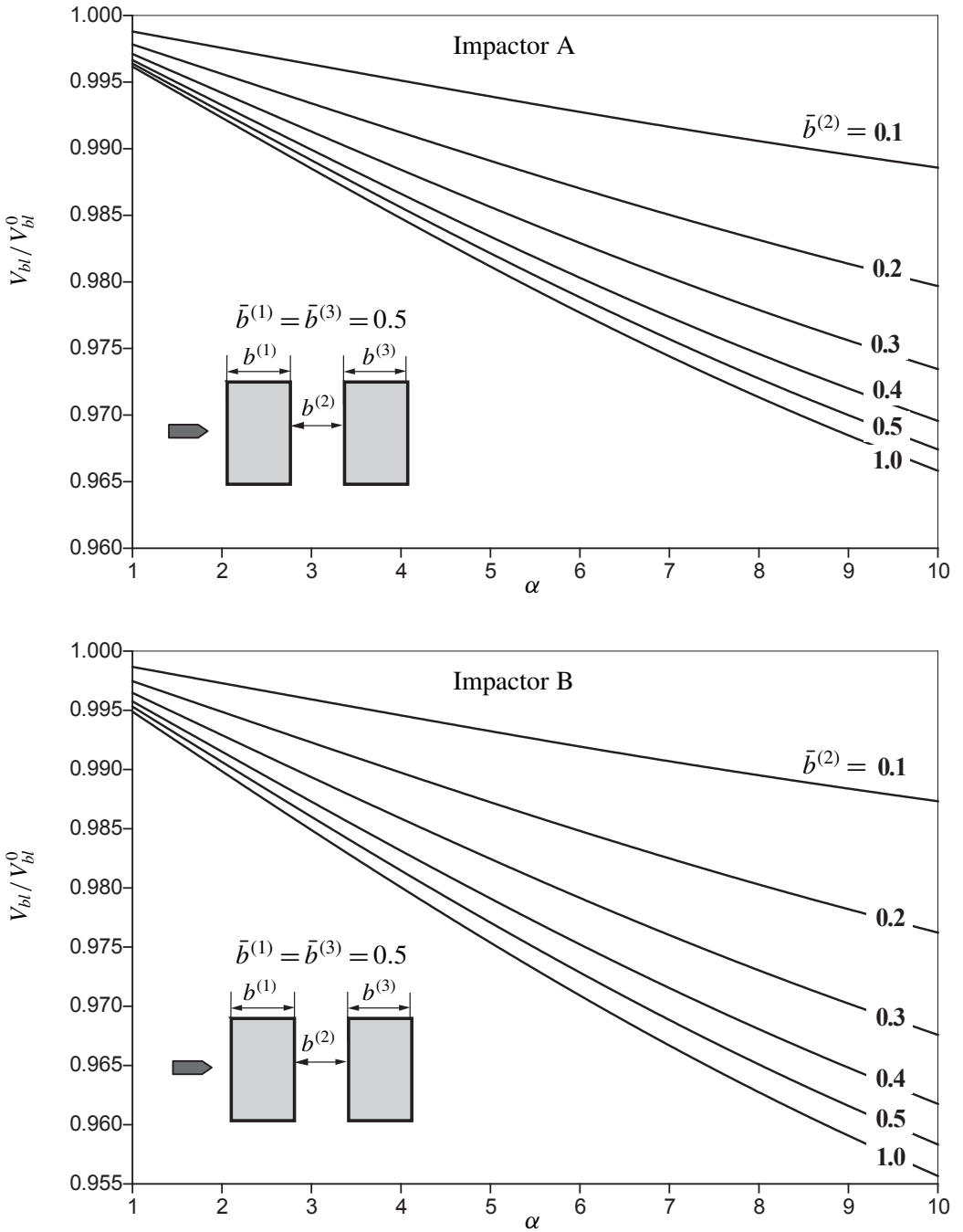


Figure 4. Effect of the thickness of the air gap on ballistic properties of a two-layer shield.

Number	Material	Dynamical hardness σ (N/m ²)	Density γ (kg/m ³)	$\chi = \sigma/\gamma$ (m ² /s ²)
1	Aluminum	$350 \cdot 10^6$	2765	$0.127 \cdot 10^6$
2	Soft steel	$1850 \cdot 10^6$	7830	$0.236 \cdot 10^6$
3	Copper	$910 \cdot 10^6$	8930	$0.102 \cdot 10^6$
4	Duraluminum	$1330 \cdot 10^6$	2765	$0.481 \cdot 10^6$

Table 1. Parameters of the model. (Based on [Vitman and Ioffe 1948]).

plates is increased (the larger is parameter $\bar{b}^{(2)}$, the lower is the curve). The rate of change of parameter δ that characterizes ballistic efficiency sharply reduces with increase of $\bar{b}^{(2)}$. Thus, for instance, inspection of Figure 4 shows that increase of $\bar{b}^{(2)}$ from 0.4 to 0.5 and from 0.5 to 1.0 is accompanied by approximately the same change of δ . The effect of gaps on δ becomes more pronounced as the parameter α increases. Analysis of Figure 5 allows us to arrive at similar conclusions. In this figure we showed the results obtained for a shield consisting of three plates whereby the widths of air gaps between the first and the second plate and between the second and the third plate are varied but remain equal. Therefore the maximum negative effect of spacing (which is the most interesting) occurs for large air gaps equal to the length of the impactor's nose since in the framework of the used model, further increase of the air gap width does not change the BLV of the shield. Our further analysis is performed exactly for this width of air gap ($\bar{b}^{(2)} \geq 1$).

In Figure 6, we show the plots of function $\delta(\alpha)$ for the case of two identical plates and for different magnitudes of the total width of the shield, \bar{b}_{sum} . Inspection of these plots shows that the effect of air gaps is more pronounced for large α . It must be noted that some curves in Figure 6 intersect, that is, for two shields with different total thicknesses parameter δ can be larger for the first shield than for a second one for one magnitude of the parameter α , and it can become smaller than for the second shield for a different value of parameter α . The same dependencies are observed in the case when a plate is separated into three identical plates with equal widths of the gaps between the plates (Figure 7).

In Figures 8 and 9, we show the plots of $\delta(\lambda)$ for $\bar{b}_{\text{sum}} = 1$ and $\bar{b}_{\text{sum}} = 2$, respectively, and for different values of parameter α (λ is the ratio of the width of the first plate to the total width, $\lambda = b^{(1)}/b_{\text{sum}}$). Inspection of these figures suggests that the shape of the impactor affects the plots only weakly, and that for every value of parameter α the curves $\delta(\lambda)$ are concave; that is, initially the increase in relative thickness of the first plate causes an increase in the negative effect of spacing, until some maximum value is attained, and then it starts to decrease; the magnitude of λ

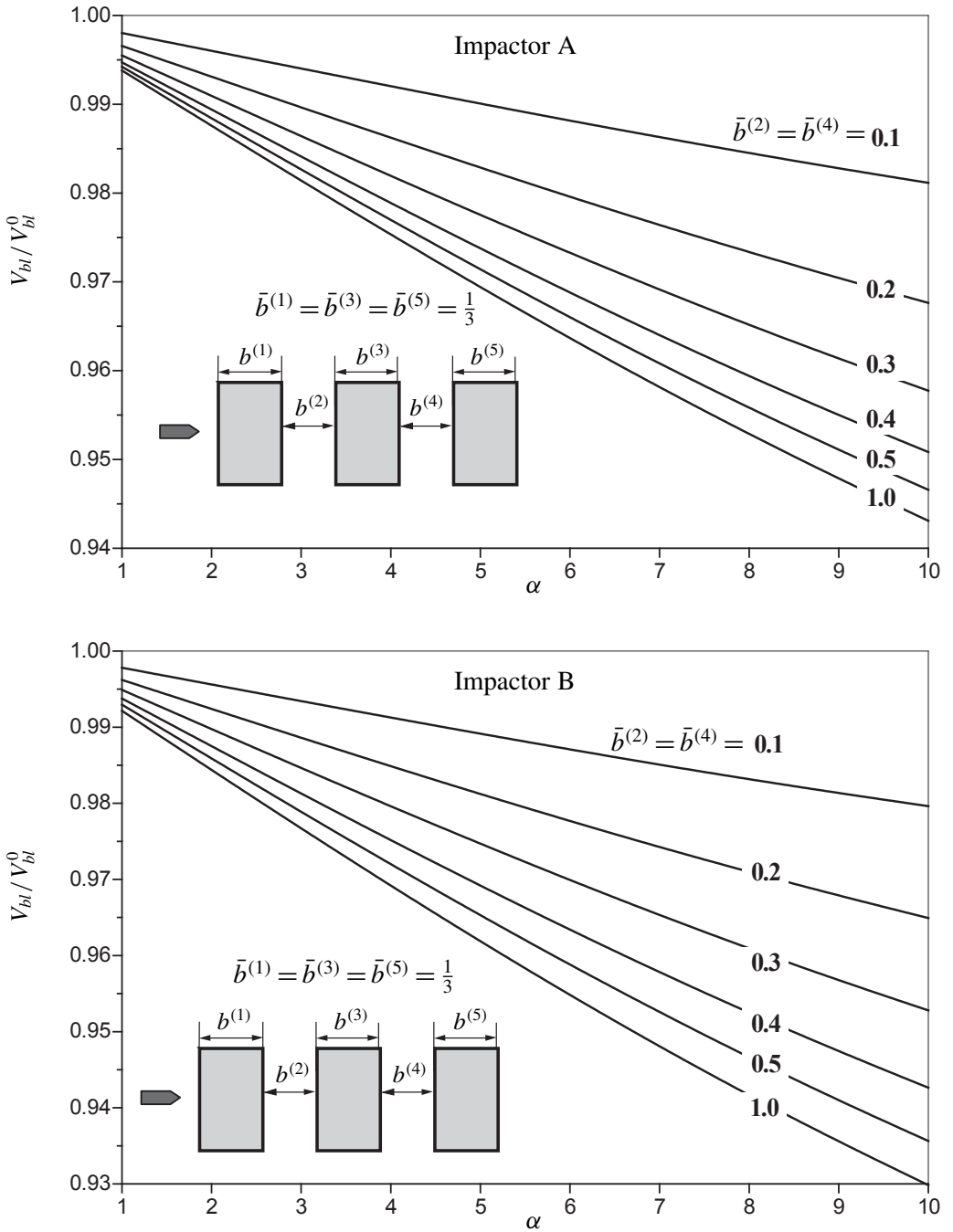


Figure 5. Effect of the thickness of the air gap on ballistic properties of a three-layer shield.

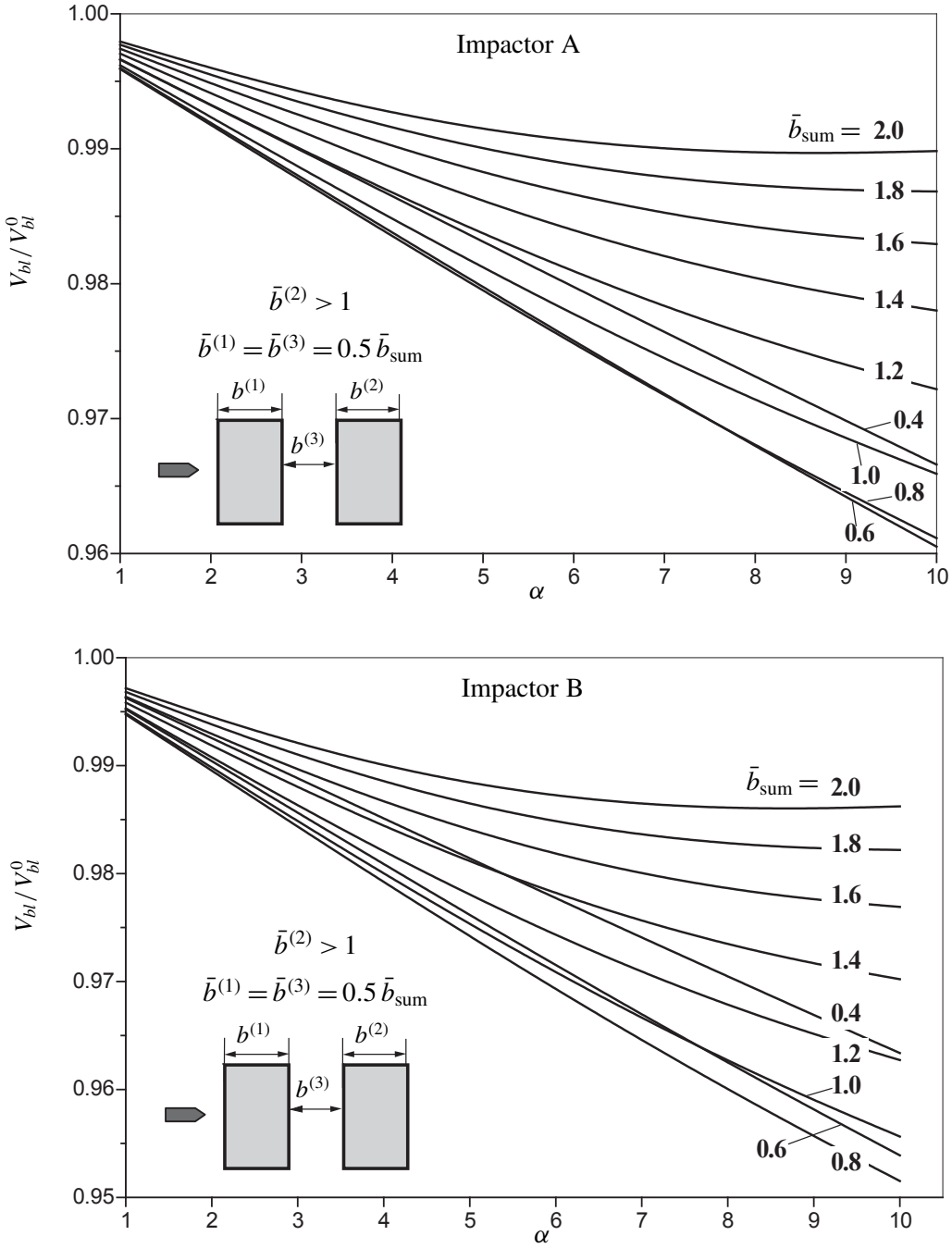


Figure 6. Effect of the parameters α and \bar{b}_{sum} on ballistic properties of two-layer shield with large air gap.

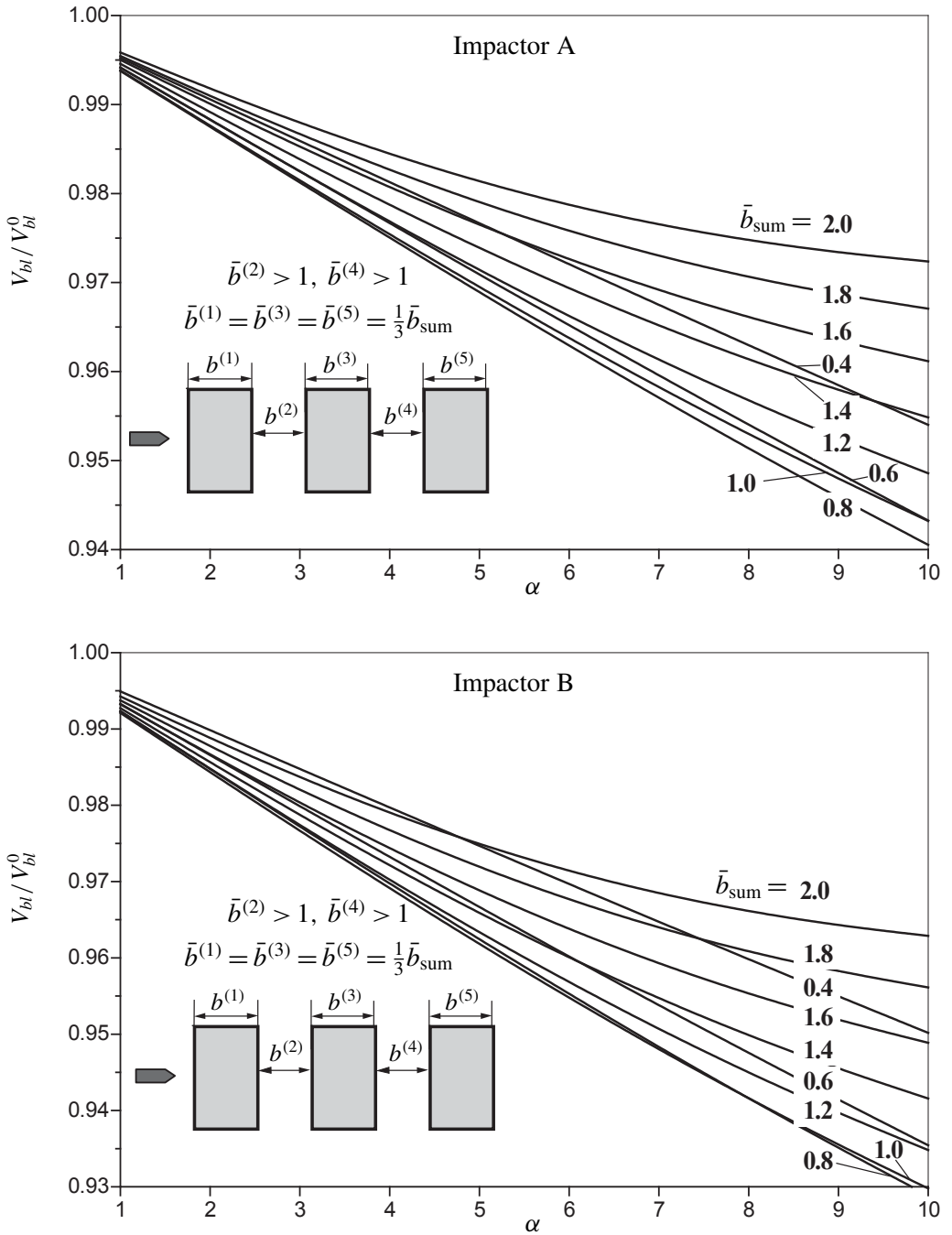


Figure 7. Effect of parameters α and \bar{b}_{sum} on ballistic properties of three-layer shield with large air gaps.

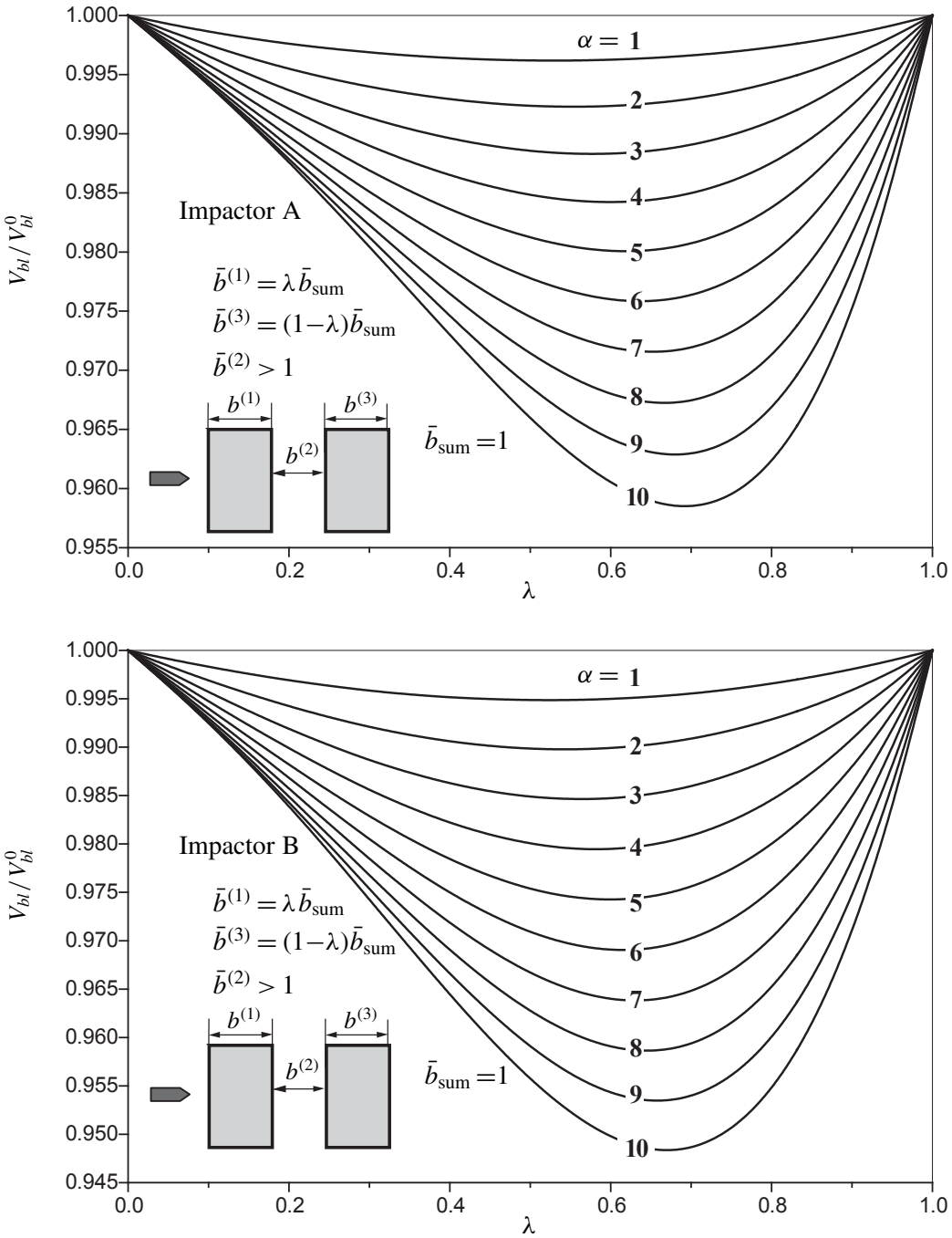


Figure 8. Effect of the thicknesses of plates on ballistic properties of two-layer shield with large air gap and $\bar{b}_{sum} = 1$.

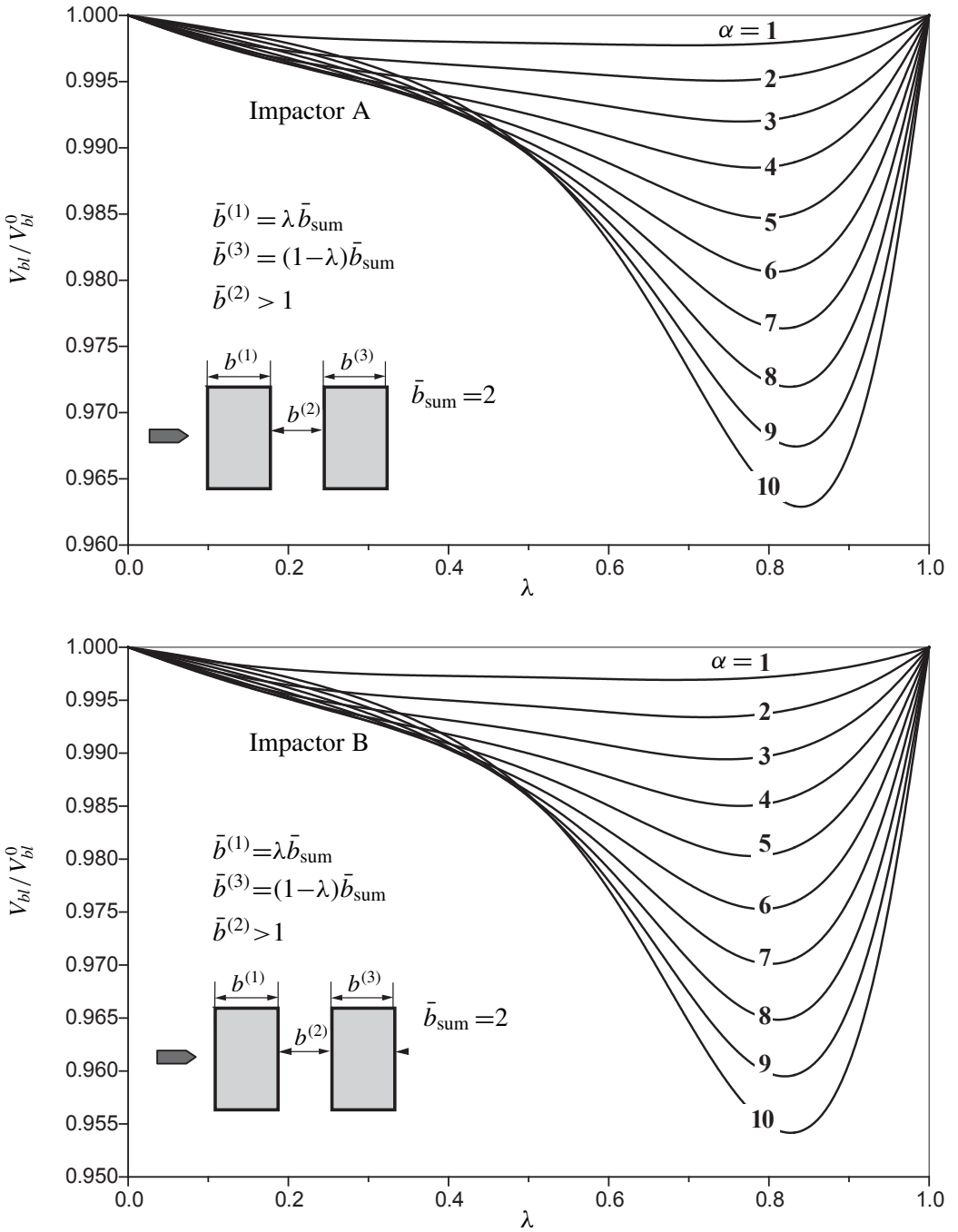


Figure 9. Effect of the thicknesses of plates on ballistic properties of two-layer shield with large air gap and $\bar{b}_{\text{sum}} = 2$.

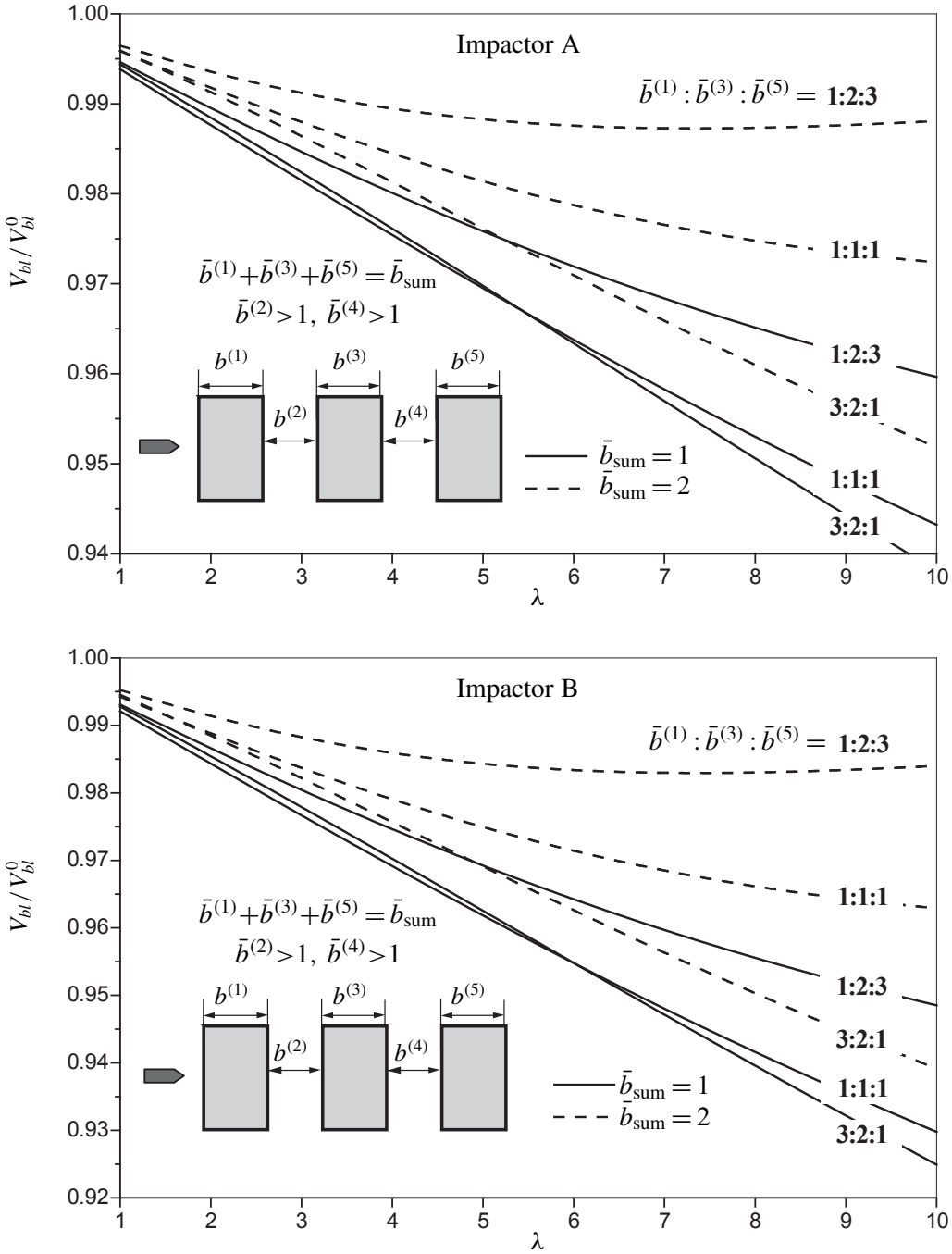


Figure 10. Effect of the thicknesses of plates on ballistic properties of three-layer shield with large air gaps.

where the negative effect of spacing is maximum depends upon the total thickness, and it increases with the increase of parameter α .

Figure 10 compares the results obtained for a spaced shield consisting of three plates with different relative thicknesses of the plates with a constant total thickness, \bar{b}_{sum} , for $\bar{b}_{\text{sum}} = 1$ and $\bar{b}_{\text{sum}} = 2$. Calculations were performed for three sets of the relative thicknesses of the plates, $b^{(1)} : b^{(2)} : b^{(3)}$, namely, 1 : 2 : 3, 1 : 1 : 1 and 3 : 2 : 1. The results show that the negative effect of spacing is minimum for configuration 1 : 2 : 3, and it depends on α for two other configurations.

Therefore, in the framework of the employed model, the effect of spacing on the BLV of the nonconical impactors is of the order of several percent. The results of the calculations showed that for slender projectiles this effect becomes even smaller.

4. Discussion of experimental results

Experimental data that allow us to compare directly the BLV of spaced shields and shields with plates in contact are not available. However we can use the results of the experiments performed with spaced and nonspaced shields for the same magnitudes of the impact velocity, v_{imp} . These data were published in [Almohandes et al. 1996] for 7.62 mm bullets perforating a mild steel shield. First, using the model, we analyze the connection between the value of energy absorbed and the value of BLV of the spaced and nonspaced shields for the same magnitude v_{imp} .

Using relationships for the impact energy E_{imp} and residual energy E_{res} of the impactor,

$$E_{\text{imp}} = \frac{1}{2} m v_{\text{imp}}^2, \quad E_{\text{res}} = \frac{1}{2} m v_{\text{res}}^2,$$

and Equation (5) rewritten as

$$v_{\text{res}}^2 = \frac{1}{q_*} [v_{\text{imp}}^2 - v_{\text{bl}}^2], \quad q_* = q(b + L) = Q(\bar{b} + 1),$$

we obtain for the relative energy absorbed by the spaced shield:

$$e_{\text{abs}} = \frac{E_{\text{imp}} - E_{\text{res}}}{E_{\text{imp}}} = \frac{q_* - 1}{q_*} + \frac{1}{q_*} \left(\frac{v_{\text{bl}}}{v_{\text{imp}}} \right)^2. \quad (7)$$

Since q_* is the same for the spaced and nonspaced shield (see below), we may write an equation similar to (7) for the spaced shield:

$$e_{\text{abs}}^0 = \frac{E_{\text{imp}} - E_{\text{res}}^0}{E_{\text{imp}}} = \frac{q_* - 1}{q_*} + \frac{1}{q_*} \left(\frac{v_{\text{bl}}^0}{v_{\text{imp}}} \right)^2.$$

Then

$$e_{\text{abs}} - e_{\text{abs}}^0 = \frac{1}{q_*} \left(\frac{v_{\text{bl}}^0}{v_{\text{imp}}} \right)^2 \left[\left(\frac{v_{\text{bl}}}{v_{\text{bl}}^0} \right)^2 - 1 \right]. \quad (8)$$

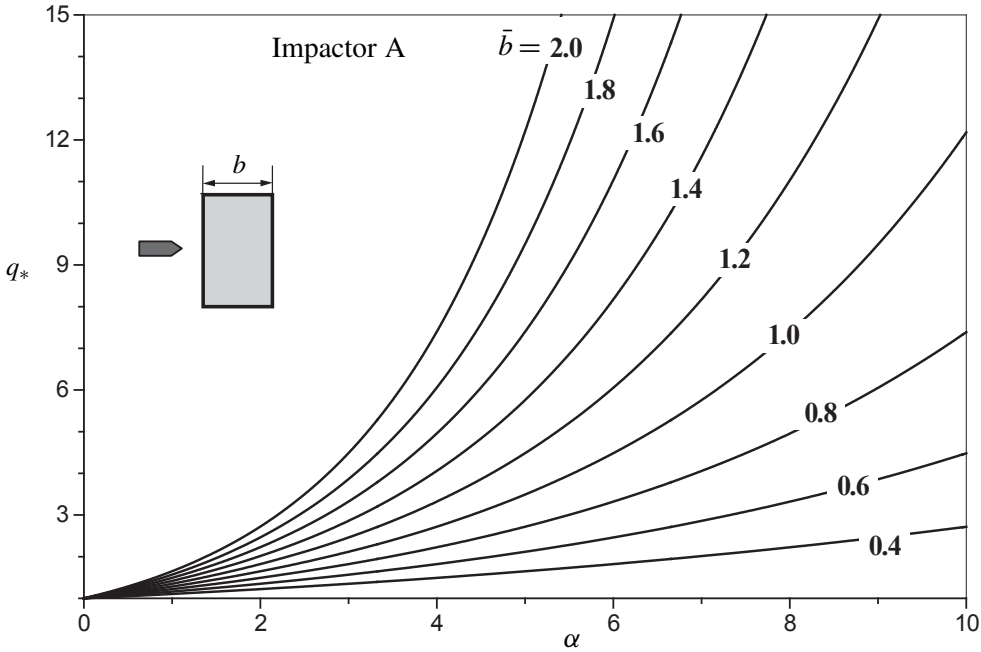


Figure 11. Function $q_*(\alpha)$ for different values of \bar{b} .

Taking into account that for $|v_{bl}/v_{bl}^0 - 1| = |\delta - 1| \ll 1$,

$$\left(\frac{v_{bl}}{v_{bl}^0}\right)^2 - 1 \equiv (\delta - 1)^2 + 2(\delta - 1) \approx 2(\delta - 1),$$

we can rewrite (8) as follows:

$$e_{abs} - e_{abs}^0 \approx k(1 - \delta), \quad k = \frac{2}{q_*} \left(\frac{v_{bl}^0}{v_{imp}}\right)^2.$$

Since $v_{bl}^0 \leq v_{imp}$ and $q_* > 1$, then $k < 2$. Moreover, when α increases, the magnitude of q_* increases (see Figure 11), which compensates for a certain increase in δ discussed above. Therefore, the model predicts insignificant change of the absorbed energy in the whole practical range of variation of parameter α . Since the predicted magnitude of the change lies within the range of experimental error and model uncertainty, it is conceivable that experimentally observed v_{bl}^0 and v_{bl} will be different by several percent, and that there will be situations when $v_{bl}^0 < v_{bl}$, and when $v_{bl}^0 > v_{bl}$. The latter conclusion is supported by the data in Table 2, compiled from experimental results of Almohandes et al. [1996]. The table shows, for each shield configuration and each impact velocity, the percent impact energy absorbed by a spaced shield, and the corresponding percentage for a shield consisting of the

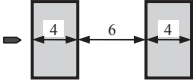
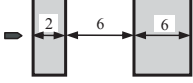
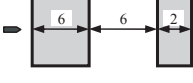
#	Structure (sizes in mm)	$v_{imp} =$				
		706.0	754.5	775.4	804.5	826.2
1		52.2	49.6	47.4	35.9	34.5
		52.5	50.0	46.5	36.1	34.8
2		54.9	52.2	50.7	42.1	37.4
		54.3	53.6	49.8	42.7	36.5
3		54.4	52.0	49.7	41.5	35.1
		55.5	52.1	51.7	41.4	37.3

Table 2. Relative energy absorption, in percent. For each structure, the top row indicates the percent absorption for the spaced shield, and the second, for a shield with plates in contact. Based on experimental results from [Almohandes et al. 1996].

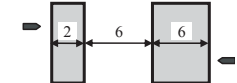
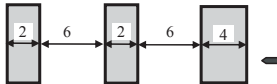
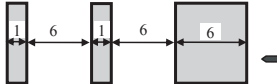
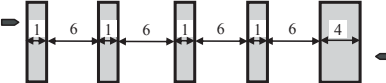
#	Structure (sizes in mm)	$v_{imp} =$				
		706.0	754.5	775.4	804.5	826.2
1		54.9	52.2	50.7	42.1	37.4
		54.4	52.0	49.7	41.5	35.1
2		51.3	49.0	44.0	33.8	32.4
		50.9	48.4	44.3	36.0	32.7
3		53.0	49.1	46.8	35.9	34.7
		54.7	54.3	52.1	37.2	36.4
4		44.2	42.3	38.4	34.0	31.5
		46.0	46.3	37.5	32.6	33.2

Table 3. Comparison of the relative energy absorption, in percent, caused by the interchange of the order of the plates. For each structure the first row describes entry from the left and the second, entry from the right. Based on experimental results from [Almohandes et al. 1996].

same plates in the same order but without air gaps. Table 3 shows that reversing the order of the plates in a spaced shield does not cause significant changes in the

absorbed energy. In the table one also observes cases where $v_{bl}^0 < v_{bl}$ and where $v_{bl}^0 > v_{bl}$.

5. Concluding remarks

Using an approximate model that takes into account the plastic deformation of the shield during perforation, we analyzed the effect of air gaps upon ballistic properties of the shield against nonconical rigid impactors. It was found that nonconical shape of the impactor causes insignificant change (in the range of several percent) of BLV and energy absorbed by a shield. The obtained results are supported by available experimental data.

References

- [Almohandes et al. 1996] A. A. Almohandes, M. S. Abdel-Kader, and A. M. Eleiche, “Experimental investigation of the ballistic resistance of steel-fiberglass reinforced polyester laminated plates”, *Compos. B: Eng.* **27**:5 (1996), 447–458.
- [Backman and Goldsmith 1978] M. E. Backman and W. Goldsmith, “The mechanics of penetration of projectiles into targets”, *Int. J. Eng. Sci.* **16**:1 (1978), 1–99.
- [Ben-Dor et al. 1998a] G. Ben-Dor, A. Dubinsky, and T. Elperin, “Effect of air gaps on ballistic resistance of targets for conical impactors”, *Theor. Appl. Fract. Mech.* **30**:3 (1998), 243–249.
- [Ben-Dor et al. 1998b] G. Ben-Dor, A. Dubinsky, and T. Elperin, “On the ballistic resistance of multi-layered targets with air gaps”, *Int. J. Solids Struct.* **35**:23 (1998), 3097–3103.
- [Ben-Dor et al. 1999] G. Ben-Dor, A. Dubinsky, and T. Elperin, “Effect of air gap and order of plates on ballistic resistance of two layered armor”, *Theor. Appl. Fract. Mech.* **31**:3 (1999), 233–241.
- [Ben-Dor et al. 2005] G. Ben-Dor, A. Dubinsky, and T. Elperin, “Ballistic impact: recent advances in analytical modeling of plate penetration dynamics, a review”, *Appl. Mech. Rev.* **58**:6 (2005), 355–371.
- [Corran et al. 1983a] R. S. J. Corran, C. Ruiz, and P. J. Shadbolt, “On the design of containment shields”, *Comput. Struct.* **16**:1-4 (1983), 563–572.
- [Corran et al. 1983b] R. S. J. Corran, P. J. Shadbolt, and C. Ruiz, “Impact loading of plates—an experimental investigation”, *Int. J. Impact Eng.* **1**:1 (1983), 3–22.
- [Elek et al. 2005] P. Elek, S. Jaramaz, and D. Mickovic, “Modeling of perforation of plates and multi-layered metallic targets”, *Int. J. Solids Struct.* **42**:3–4 (2005), 1209–1224.
- [Gupta and Madhu 1997] N. K. Gupta and V. Madhu, “An experimental study of normal and oblique impact of hard-core projectile on single and layered plates”, *Int. J. Impact Eng.* **19**:5–6 (1997), 395–414.
- [Honda et al. 1930] K. Honda, G. Takamae, and T. Watanabe, “On the measurement of the resistance of shield plates to penetration by a rifle bullet”, *Tohoku Imperial Univ. Ist Ser.* **19** (1930), 703–725.
- [Hurlich 1950] A. Hurlich, “Spaced armor”, Report WAL-710/930-1, Watertown Arsenal Lab., MA, 1950.
- [Kamke 1959] E. Kamke, *Differentialgleichungen: Lösungsmethoden und Lösungen — gewöhnliche Differentialgleichungen*, Geest und Portig, Leipzig, 1959.

- [Liang et al. 2005] C.-C. Liang, M.-F. Yang, P.-W. Wu, and T.-L. Teng, "Resistant performance of perforation of multi-layered targets using an estimation procedure with marine application", *Ocean Eng.* **32**:3-4 (2005), 441-468.
- [Marom and Bodner 1979] I. Marom and S. R. Bodner, "Projectile perforation of multi-layered beams", *Int. J. Mech. Sci.* **21**:8 (1979), 489-504.
- [Radin and Goldsmith 1988] J. Radin and W. Goldsmith, "Normal projectile penetration and perforation of layered targets", *Int. J. Impact Eng.* **7**:2 (1988), 229-259.
- [Recht 1990] R. F. Recht, "High velocity impact dynamics: analytical modeling of plate penetration dynamics", pp. 443-513 in *High velocity impact dynamics*, edited by J. A. Zukas, Wiley, New York, 1990.
- [Vitman and Ioffe 1948] F. F. Vitman and B. S. Ioffe, "A simple method of determining the dynamical hardness of metals using a double cone", *Zavodskaja Laboratorija* **14**:6 (1948), 727-732. In Russian.
- [Vitman and Stepanov 1959] F. F. Vitman and V. A. Stepanov, "Effect of the strain rate on the resistance of metals to deformation at impact velocities of 100-1000 m/s", pp. 207-221 in *Nekotoryie problemy prochnosti tvordogo tela*, USSR Acad. of Sci., Moscow and Leningrad, 1959. In Russian.
- [Zukas 1996] J. A. Zukas, "Effect of lamination and spacing on finite thickness plate perforation", pp. 103-115 in *Structures under shock and impact, IV*, edited by C. A. B. N. Jones and J. A. Watson, Comput. Mech. Publ., Southampton, 1996.

Received 15 Oct 2005. Revised 6 Dec 2005.

GABI BEN-DOR: bendorg@bgu.ac.il

Department of Mechanical Engineering, Ben-Gurion University of the Negev, POB 653, Beer-Sheva 84105, Israel

ANATOLY DUBINSKY: dubin@bgu.ac.il

Department of Mechanical Engineering, Ben-Gurion University of the Negev, POB 653, Beer-Sheva 84105, Israel

TOV ELPERIN: elperin@bgu.ac.il

Department of Mechanical Engineering, Ben-Gurion University of the Negev, POB 653, Beer-Sheva 84105, Israel

